EFFECTIVENESS OF SHOT PEENING IN SUPPRESSING FATIGUE CRACKING AT NON-METALLIC INCLUSIONS IN UDIMET® 720

R. L. Barrie[1], T. P. Gabb[2], J. Telesman[2], P. T. Kantzos[3], A. Prescenzi[4], T. Biles[5], P. J. Bonacuse[6]

[1]US Army Aviation and Missile Command, Redstone Arsenal, AL 35898-5000
[2]NASA Glenn Research Center, 21000 Brookpark Rd., Cleveland, OH 44135-3191
[3]Honeywell Engine Systems, PO Box 29003, Phoenix, AZ 85038-9003
[4] Ohio State University, 2041 College Rd., Columbus, OH 43210
[5]Alcoa Wheel and Forged Products, 1600 Harvard Ave., Cleveland OH, 44105
[6]Army Research Laboratory, NASA GRC, 21000 Brookpark Rd., Cleveland OH, 44135-3191

Abstract

The fatigue lives of modern powder metallurgy disk alloys can be reduced over an order of magnitude by cracking at inherent non-metallic inclusions. The objective of this work was to study the effectiveness of shot peening in suppressing LCF crack initiation and growth at surface nonmetallic inclusions. Inclusions were carefully introduced at elevated levels during powder metallurgy processing of the nickel-base disk superalloy Udimet 720. Multiple strain-controlled fatigue tests were then performed on machined specimens with and without shot peened test sections at 427°C and 650°C. The low cycle fatigue lives and failure initiation sites varied as functions of inclusion content, shot peening, and fatigue conditions. A large majority of the failures in as-machined specimens with the introduced inclusions occurred at cracks initiating from inclusions intersecting the specimen surface. These inclusions reduced fatigue life by up to 100X,

when compared to lives of material without inclusions residing at specimen surface. Large inclusions produced the greatest reductions in life for tests at low strain ranges and high strain ratios. Shot peening improved life in many cases by reducing the most severe effects of inclusions.

Keywords: Shot peening, fatigue, inclusions, superalloy, disk

Introduction

The low cycle fatigue (LCF) lives and predominant failure modes of powder metallurgy (PM) nickel-base superalloy compressor and turbine disks can be influenced by material processing details including powder characteristics, consolidation, extrusion, forging, heat treating, and machining processes[1]. Among these variables, the effects of inherent non-metallic inclusions introduced during the powder production and handling have been shown to often limit LCF life [1-12].

A comprehensive review of early efforts concerning this issue is presented in reference 1. Tests of early powder metallurgy superalloys [2, 3] showed enhance fatigue crack initiation occurred at inclusions for both room and high temperature conditions. Inclusion morphology, size, shape, and location were shown to influence fatigue life. Thermal mechanical processing of disk superalloys after consolidation has improved fatigue response by breaking up inclusions to some degree. Modern nickel disk powder processing facilities have also successfully reduced inclusion contamination to extremely low levels [4]. However, the quantities of full scale compressor and turbine disks produced have sufficient collective volume and surface area that these rare inclusions can

be present at high stress locations. A more recent study [5] of a modern disk superalloy Rene 88DT used purposefully introduced ("seeded") elevated levels of carefully controlled inclusions before consolidation and thermal mechanical processing, in order to allow enough inclusions to occur within samples for their effects to be closely studied. Test results here indicated life reductions due to the seeds of 28-95% compared to unseeded material, with larger inclusions producing lower lives at equivalent test conditions, and greater life reductions in tests at high temperature, 649°C. In that study, some specimens were shot peened after machining, to simulate fully processed disk surfaces. The shot peening reportedly produced compressive residual stresses near the specimen surface, which sometimes improved the fatigue lives of seeded specimens. Only a single set of shot peening conditions was apparently applied there. Work on this and other superalloys with careful interrupted testing [6] and in-situ testing with scanning electron microscopes [7] have shown cracks can initiate at surface-connected inclusions very early in fatigue cycling, to cause premature failure. This helped explain why in numerous investigations for fixed fatigue test conditions, surface-initiated failures produced significantly lower fatigue lives than internally initiated failures. However, in certain fatigue conditions, an incubation period of cycling was reported necessary before crack initiation commenced, so that crack propagation life calculations could not fully account for observed fatigue lives [5, 6]. The referenced work indicates the effects of inclusions residing at such locations on fatigue life could be quite substantial, especially in tests at high temperatures.

Shot peening is a surface enhancement process which produces beneficial compressive residual stresses on metallic surfaces [8]. This process has been adopted to

improve the fatigue life of nickel-base disk superalloy components by reducing the propensity for cracks to initiate at machined surfaces. However, shot peening plastically deforms the surface material which produces microstructural damage and consumes ductility, so shot peening conditions must be carefully screened for fatigue applications. The potential exists for shot peening to be specifically applied to reduce the effects of surface inclusions on fatigue life of disk superalloys [5]. However, shot peening conditions have not usually been optimized to specifically address this particular issue.

The objective of this work was to study the effectiveness of shot peening in suppressing LCF crack initiation and growth at surface nonmetallic inclusions in a powder metallurgy processed disk superalloy, Udimet 720. When powder metallurgy processed and subsolvus heat treated to produce a fine grain size near 10 μm, this superalloy is often limited in fatigue cycling by cracking at nonmetallic inclusions [9]. However, since natural inclusions occur so infrequently on specimen surfaces, elevated levels of nonmetallic inclusions were introduced before consolidation at carefully controlled quantities and sizes into Udimet 720 powder having very low inherent inclusion content [10]. This "seeded" powder was then hot isostatically pressed, extruded, isothermally forged into subscale disks, and heat-treated. The LCF lives of specimens machined from the seeded subscale disks were compared to those also given shot peening as well as specimens from unseeded disks, in fatigue tests at 427°C and 650°C.

Materials and Procedures

Material Processing

Udimet 720 (U720) powder was atomized in argon at Special Metals Corporation, Inc. This powder was produced and handled using state-of-the-art full-scale production practices to minimize powder contamination of any nature. The powder was then sieved through a -270 mesh screen and divided into three portions. Two portions were seeded with alumina particles, and one portion was consolidated in its unseeded condition.

The seeds were designed to behave in a similar manner to inclusions that are inherently present in conventionally processed powder. A sufficient quantity of seeds was added and fully blended in the superalloy powder to ensure that several inclusions would intersect the gage surface of each LCF test specimen [10]. One portion of powder was seeded with small inclusions, having an approximate median diameter of 54 μm and median projected area of 2,316 μm^2, produced by crushing pre-baked Ram 90 alumina crucible paste. A second portion of powder was seeded with relatively large inclusions, having an approximate median diameter of 122 μm and median projected area of 11,700 μm^2, made of crushed Alcoa T64 alumina, a common crucible material. The third portion of superalloy powder was retained in its natural or unseeded condition to provide a baseline for comparison.

Three separate stainless steel cans were filled with the three powder portions, then consolidated using the same processing conditions and procedures. The three portions of powder were hot isostatically pressurized, extruded, and forged into disks approximately 17.5 cm in diameter and 4 cm thick. The disks were then heat treated in a gas-fired furnace at Wyman-Gordon Forgings, Inc., in mixed groups of four arranged in a consistent square array on a superalloy tray. The subsolvus solution heat treatment was

performed at 1120°C for three hours. Each tray of disks was then transferred in about 1 minute to a tank containing agitated oil held at a temperature of about 50°C. The disks were subsequently given aging heat treatments of 760°C for 8 hours, followed by 650°C for 24 hours. The resulting subsolvus microstructures of the unseeded and seeded disks were quite comparable, Fig. 1. The average grain size was approximately 8 μm, equivalent to ASTM 11. Undissolved primary gamma prime (γ′) as well as dissolved and precipitated cooling and aging γ′ precipitate contents and sizes were all comparable between the unseeded and seeded disks. The seeded inclusions were often broken up and then stretched by the extrusion and forging processes, respectively, producing elongated and flattened ellipsoid-like morphology having lengths up to twice the maximum lengths of the original inclusions [11, 12]. This effect was more pronounced for the 54 μm seeded inclusions, as also shown in Fig. 1.

Specimen blanks were extracted by electro-discharge machining from the unseeded and seeded disks. The specimen sizes were designed to influence occurrence probabilities for the inclusions. For the unseeded material, smaller specimens were tested to minimize the probability of a natural inclusion intersecting the specimen surface. For the seeded material, larger specimens were used to give sufficient probability of several seeded inclusions intersecting the specimen surface. Blanks 1.42 cm diameter and 5.33 cm long were machined from the unseeded disks, aligned circumferential to the pancake centerline. Blanks 1.98 cm diameter and 8.26 cm long were machined from the seeded disks, aligned in the same manner. Sections of Inconel 718 were inertia welded to the ends of each blank and the resulting assemblies were then machined by low stress grinding into low cycle fatigue specimens with the desired gage section dimensions

(Table I). Previous testing of another disk superalloy without seeded inclusions indicated these two specimen configurations give comparable fatigue lives [13].

Shot peening was performed according to AMS 2432 specifications, and included intensity and coverage calibrations, nozzle and specimen masking, and appropriate process controls. Metal Improvement Corp. performed the shot peening using conditioned cut stainless steel wire of 360 μm mean diameter (0.014 in., CCW14 designation). Fatigue specimens were rotated in a fixture while a nozzle maintained at a constant angle was translated to apply the shot at constant angle, distance, pressure and flow rate, using a computer controlled automated system. Initial screening to determine appropriate shot peening conditions was performed at extremes of 4 and 8 Almen (A) intensities and coverages of 200% and 800%, as well as several intermediate coverages at an intermediate intensity of 6A, Table II. Residual stress and x-ray peak width were measured as functions of depth on screening specimens by Lambda Technologies [14]. To generate these depth profiles, specimen surfaces were repetitively x-rayed, then electropolished to remove a measured layer of material. The stresses were adjusted to account for removal of the previously constraining layer. Peak width was independently calibrated with measurements on plastically deformed compression specimens, in order to estimate cold work in the shot peened specimens. Metallographic sections were prepared transverse to shot peened surfaces for evaluations of the number of laps per linear surface width. A lap was defined as any location where material was folded over itself on the surface. The inclusions intersecting several specimen surfaces were mapped and evaluated before and after shot peening, to determine the degree of material lapping

over inclusions. Fig. 2 shows representative plots and images of the parameters monitored for this study.

Mechanical Testing

Fatigue tests were performed at 427°C and 650°C in closed-loop servo-hydraulic testing machines using induction heating and axial extensometers. Initial LCF tests to screen and select shot peening conditions were performed LCF testing at 650°C with a total strain range ($\Delta\varepsilon_t$) of 0.8%, and a strain ratio (R_ε = minimum strain/maximum strain) of zero on the two seeded materials, using the large gage LCF specimen. Subsequent LCF evaluations were performed at 427 and 650°C using several total strain ranges and strain ratios of –1, 0, and 0.5. Each fatigue test was performed in two stages to reduce total testing time. For the first 24 hours, the test was conducted with strain controlled using a triangular waveform at a frequency of 0.33 hertz to produce a constant total strain range ($\Delta\varepsilon_t$). After cycling for 24 hours, tests were continued to failure with load controlled using a triangular waveform at a frequency of 5 hertz to maintain the stabilized maximum and minimum stresses for each specimen, at a frequency of 5 hertz. Past testing has shown that the change in control mode has negligible effects on fatigue life in these conditions. All tests were continued to failure, and fractographic evaluations were performed on all specimens to determine the failure initiation sites.

Results and Discussion

Screening Tests of Shot Peening Conditions

Shot peening conditions were first screened using test specimens and fatigue tests at 650°C with $\Delta\varepsilon_t$=0.8% and R_ε=0 to ascertain optimal shot peening conditions for seeded material. Screening tests were performed for shot peening condition extremes of 4 Almen (A) and 8A intensities, and coverages of 200 and 800%, and at 6A with intermediate coverages (Table II). After shot peening and prior to mechanical testing, measurements were made of the surface and maximum compressive residual stresses, depth of compression, peak width, laps per linear surface length, and the ratio of exposed inclusion surface area after/before shot peening for each shot peening condition. A representative surface residual stress plot indicating the various measured residual stress responses is shown in Fig. 2. Simple scatter plots of each of the measured responses are shown versus the peening variables in Fig. 3. Maximum compressive residual stresses just exceeding 1000 MPa were produced in all cases. The surface compressive residual stress and peak width varied more with shot peening intensity and coverage. Linear variations of compression depth and surface peak width were evident; however, the relationships with other responses appeared less clear. Laps per linear surface length showed strong variations with intensity and coverage, while the ratio of exposed inclusion surface areas measured after/before shot peening showed smaller variations

The resulting fatigue lives are shown versus intensity and coverage for each seeded material in Fig. 4. Unseeded, shot peened specimens were not evaluated for fatigue life in this study. Life did not strongly vary with intensity and coverage for specimens with 54 μm seeds, but varied appreciably for specimens with 122 μm seeds.

All of the 54 and 122 μm seeded specimens without shot peening failed from cracks initiating at surface inclusions. Shot peening at all combinations of conditions successfully suppressed this failure mode for the 54 μm seeded material, such that cracks initiating from internal inclusions caused failure. This was consistent with their significantly improved LCF lives over unpeened specimens. However, crack initiations at surface inclusions were not so easily suppressed for 122 μm seeded material. In most combinations of shot peening conditions, cracks still initiated from surface inclusions to cause failures as in untreated specimens. Only the high intensity, low coverage combination of 8A/200% succeeded in suppressing this cracking mode, such that the failures initiated from cracking at internal inclusions. These internal failure initiations resulted in a significant improvement in fatigue life for this condition.

In order to clearly assess and compare the effects of shot peening variables on the responses, multiple linear regression was performed on each of the responses, using forward and reverse stepwise selection of the variables intensity (I), coverage (C), and specimen diameter (D) where applicable. The variables (V) were first standardized using Equation 1.

$$V' = \frac{(V - V_{mid})}{(V_{range}/2)} \tag{1}$$

A 95% probability of significance was required for inclusion of any variable. The resulting relationships are listed along with the number of data points (n), residual degrees of freedom (resDoF), residual root mean square error (RMS error), and correlation coefficient adjusted ($R^2_{adj.}$) for the variables in Table III. The correlation

coefficient ($R^2_{adj.}$) was used as a measure of the applicability of the regression, with $R^2_{adj.}$ ≥0.25 indicating ≥50% of the response variation is accounted for by the regression equation. Analysis of the screening test data reveals the following trends:

1. The maximum compressive residual stress was very stable and did not vary significantly as a function of shot peening conditions.
2. Stress on the shot peened surface was less compressive with increasing intensity.
3. The surface x-ray peak width and corresponding cold work level increased with increasing coverage.
4. The depth of compressive stresses increased with increasing intensity and specimen diameter.
5. The laps/cm increased with increasing intensity, coverage, and specimen diameter. Correspondingly, the ratio of exposed inclusion area decreased with increasing intensity, coverage, and specimen diameter.
6. Fatigue life of 54 μm seeded material was significantly improved for all combinations of shot peening conditions. This was consistent with the shift to internal failure initiations for all peening conditions. However, life moderately decreased with increasing coverage, suggesting the corresponding increased cold work consumed some ductility and crack initiation life.
7. A more complicated interactive relationship of intensity and coverage with fatigue life was observed for the 122 μm seeded material. Life increased with the combination of either high intensity and low coverage, or low intensity with high coverage.

These trends reflected the interrelationships among these various shot peening parameters and the fatigue crack initiation tendencies at surface inclusions. All

combinations of shot peening conditions gave sufficient compressive residual stresses to depths beyond the 54 μm surface inclusions. Consequently, all screened peening conditions allowed failure initiations at only internal 54 μm inclusions, with greatly improved life. However, only shot peening at high intensity produced compressive stresses to depths greater than the 122 μm inclusion diameter, to potentially suppress cracking at these surface inclusions. Yet, increased coverage here could override this benefit, by producing too much cold work, lapping, and other material damage near the surface to still allow cracking at these surface inclusions.

The regressed screening test results were used to project all shot peening and fatigue life responses for various shot peening conditions. Intensities of 4-6A combined with 200-400% coverage gave attractive responses at the specimen surface: high magnitude compressive stresses, low cold work, and less lapping. However, the beneficial compressive residual stresses extended only 140-200 μm into the specimen depth, and couldn't suppress fatigue cracking at 122 μm surface inclusions. Only the high intensity/low coverage condition of 8A/200% appeared to provide the necessary balance of high depth of compressive residual stresses combined with sufficient compressive stress, low cold work, and moderate lapping at the surface to suppress the surface inclusion cracking mode for the larger 122 μm seeded inclusions. Therefore, shot peening conditions of 8A intensity and 200% coverage were selected for further evaluations of effects on LCF strain-life response for seeded material.

Shot Peening Effects on Strain-Life Response at 8A Intensity and 200% Coverage

Fatigue testing was performed to determine the effectiveness of the selected shot peening condition. Testing results are summarized in Fig. 5 with plots of LCF life versus total strain range. Lives at 427°C and 650°C for strain ratios of -1, 0, and 0.5 are compared for unseeded, 54 μm seeded, and 122 μm seeded results in either unpeened or 8A/200% shot peened conditions. Fractography was performed on all specimens to determine whether each failure initiated at a surface or internal failure origin, which is indicated by open or solid symbols, respectively.

For the unpeened specimens, the lives of seeded specimens were invariably lower than for unseeded specimens. The 122 μm inclusions reduced life more than the 54 μm inclusions for fixed test conditions at 650°C. However, the two seed sizes produced similar reduced lives at 427°C. For a given strain ratio, the inclusions reduced lives on a percentage basis more at lower strain ranges than for high strain ranges. For a given strain range, unseeded and seeded specimen lives were lower at positive strain ratios. Inclusion effects on life were thereby maximized in tests at the lowest strain range of 0.6% and the most positive strain ratio of 0.5. In these conditions at 650°C, small seeds reduced life by approximately 20X, while larger seeds dramatically reduced life by 100X. The large reductions in life were associated with a shift in failure mode for seeded specimens to failures initiating from inclusions at the specimen surface, Fig. 6-8.

For the shot peened specimens tested at strain ranges of 0.6% and 0.8% with strain ratios of −1 and 0, shot peening improved life at both 427°C and 650°C by between 2X and 9X. Shot peening successfully suppressed surface cracking at inclusions in these test conditions, with failures usually initiating at internal inclusions as seen in

Fig. 7 and 8 for tests at 650°C. The greatest improvements in lives of seeded materials were observed at these conditions. The failure mode changed from cracking at surface inclusions for unpeened specimens to internal inclusions for shot peened specimens. It is interesting to note that although life was extended by peening at these conditions, the observed lives of the peened, seeded specimens did not fully attain the lives of the unpeened, unseeded specimens. The longer lives observed for peened specimens were about midway between seeded and unseeded lives for the same test conditions.

Several factors may explain why the internally initiated failures of shot peened, seeded specimens occurred at lower lives than that of the unpeened, unseeded specimens. The presence of many more inclusions throughout the gage volume of the seeded specimens allowed fatigue damage to occur and compete at numerous inclusions. Cyclic damage was presumably most accelerated by the largest, most harmfully shaped and oriented inclusion, which therefore controlled life. This is supported by the trend that lives increased in the material order: 122 μm seeded, 54 μm seeded, followed by unseeded material. As expected, the corresponding sizes of inclusions initiating these failures usually increased with the reverse material order: unseeded, 54 μm seeded, followed by 122 μm seeded materials. Furthermore, tensile residual stresses are present in the interior of the shot peened specimens as a consequence of the compressive residual stresses near the surface. Longitudinal compressive residual stresses near the surface were found in the x-ray stress profiles to be balanced by internal longitudinal tensile elastic stresses, generated to maintain static equilibrium, Fig. 2. This would result in a higher mean strain and stress at internal inclusions for shot peened specimens than for unpeened specimens during fatigue cycling.

At a high strain ratio of R_ε=0.5, surface cracks at inclusions often still caused failure regardless of surface peening. Surface cracking was suppressed by shot peening here at the lowest strain range of 0.6% for 54 μm inclusions, but not for the larger 122 μm inclusions. Surface cracking at both inclusion sizes caused failure at a strain range of 0.8%. At a strain range of 1.2%, shot peening did not significantly improve life and could not suppress surface cracking at inclusions for any of the strain ratios. At total strain ranges of 0.8% and 1.2%, the high maximum strains and stresses induce plastic strains of approximately 0.2% and 0.3%, respectively, on the first fatigue cycle. X-ray diffraction measurements of the residual stresses on specimens before and after testing to failure at 650°C, $\Delta\varepsilon_t$=0.8%, and R_ε=0 indicate the majority of the beneficial compressive residual stresses produced by shot peening near the surface were eliminated by testing, Fig. 9. The evolution of these compressive residual stresses in the presence of high cyclic strains as well as high temperatures needs to be understood and modelled [15-17].

Many disk applications require low cycle fatigue lives of at least 15,000-30,000 cycles. During service, stabilized cyclic strain ranges would be expected to not exceed 0.8%, in order for the disk to have sufficient life without considering inclusion effects. In such conditions, shot peening was effective in suppressing cracking at surface inclusions, for strain ratios of 0 to –1. Therefore, shot peening could be used to minimize the effects of inclusions intersecting the surface at critical disk locations in such cases, provided the strain ratio is not too high.

Remaining Issues

The results indicate shot peening can be optimized to reduce the effects of inclusions intersecting the surface of disk alloy specimen surfaces. However, additional issues must be addressed to implement such an approach for disk applications:

1) The processes of cyclic crack initiation and crack propagation at surface inclusions need to be separated through interrupted testing of additional specimens. This would allow modeling of the effects of shot peening induced residual stresses on each of these processes, for a more accurate understanding of how shot peening could be used to improve life. Previous work [5, 6, 7] has shown that crack initiation at surface inclusions often occurs very early during fatigue cycling, but potentially could offer some "incubation" initiation life in certain cases. Early results indicate fatigue cracks can often initiate early in fatigue cycling even of shot peened specimens, but don't all continue to grow at the same rates [15]. It may be necessary to further screen and optimize shot peening conditions specifically to improve these aspects of crack initiation and early growth.

2) The effects of thermal exposure and cyclic overstrains on the compressive residual stresses introduced near the surface by shot peening must be understood. Thermal relaxation could greatly reduce the magnitude and beneficial effects of the compressive residual stresses [16, 17]. Cyclic strains and overstrains could in some conditions eliminate the compressive stresses, or even reverse the residual stresses to produce harmful tensile stresses there, Fig. 9.

3) Shot peening effects on life and surface inclusion cracking tendencies need to be evaluated for various disk machining processes. Disk machining processes including

point turning, milling, broaching, and drilling are often followed by shot peening, and could produce different residual stress and cold work profiles from those encountered here, as well as different surface roughness and irregularities [18]. These factors could influence associated fatigue lives and failure modes.

(4) The effects of realistic disk features, volumes, and stress states need to be evaluated. Blade slots and bolt holes can be subjected to mutiaxial stress states producing high, but concentrated stresses and strains at critical locations. The intersections of inclusions with these surfaces would require probabilistic simulations [12]. The cyclic stress-strain response and relaxation of material at such locations can be constrained by larger surrounding volumes of elastically loaded material in disks. The benefits of shot peening need to be evaluated for these more complex and relevant cases. This may ultimately require cyclic spin testing of appropriately treated disk test articles.

5) While optimizing peening conditions to mitigate surface initiation from inclusions, care must be taken to ensure that the peening conditions do not adversely affect the LCF behavior of the base material by introducing a large amount of coldwork damage. This did have an effect on the lives of shot peened seeded specimens in the current study. Screening of shot peening conditions with both seeded and unseeded fatigue test specimens may be necessary for optimal results.

(6) Alternative surface enhancement processes such as low plasticity burnishing [16] should be assessed for suppressing fatigue cracking at inclusions. These processes potentially offer compressive residual stresses to a greater depth than shot peening, with less cold work. Thermal relaxation of residual stresses has been shown to be accelerated

with increasing cold work [16], therefore these processes having reduced cold work could produce compressive residual stresses that are more resistant to thermal relaxation.

Summary of Results and Conclusions

The effectiveness of shot peening in suppressing LCF crack initiation and growth at surface nonmetallic inclusions was evaluated in the powder metallurgy disk superalloy Udimet 720. Initial tests of unpeened specimens indicated up to 100X reduction in fatigue lives due to failures initiating from surface inclusions. Shot peening conditions were therefore specifically screened and selected to suppress this failure mode. High intensity, low coverage conditions successfully suppressed surface inclusion cracking, and improved fatigue life in the screening tests. Subsequent LCF tests of shot peened, seeded material specimens indicated these improvements were possible at both 427 and 650°C, for strain ranges up to 0.8% and strain ratios of –1 and 0. The initial cyclic plastic strains generated at higher strain ranges and strain ratios apparently reduced the magnitude of shot peening's compressive residual stresses sufficiently to eliminate these improvements.

It can be concluded from this work that:

1) Shot peening can be used to reduce the harmful effects of surface inclusions on disk fatigue life in some conditions.

2) However, the stresses generated at surface inclusions during fatigue cycling at high strains and strain ratios can reduce the magnitude and effectiveness of the compressive stresses, such that surface cracking at inclusions can still occur in these conditions, especially for relatively large inclusions.

3) Therefore, the evolution of surface stresses introduced by shot peening needs to be measured and modeled for optimal shot peening process design, to suppress fatigue cracking at surface inclusions.

4) This evolution of these stresses may need to be combined with probabilistic considerations of potential for inclusion size and location near/at high stress locations and surfaces, to assess whether the shot peening stresses will sufficiently suppress the chances of surface cracking at inclusions.

5) The effects of thermal relaxation, overstrains, machining processes, and disk features on the stresses and inclusions may also need to be quantified, in order to realistically assess surface inclusion cracking tendencies on actual disks.

Acknowledgements

The authors wish to acknowledge the work of Tony Banik of Special Metals Corp. in powder processing, William Konkel of Wyman-Gordon-PCC, Inc. in disk processing, David Markgraf and Dan Richardson of Metal Improvement Corp. in shot peening.

References

[1] Chang , Krueger and Sprague Superalloy Powder Processing, Properties and Turbine Disk Applications. Superalloys 1984: Proceedings of the Fifth International Symposium on Superalloys. Gell M, Kortovich CS, Bricknell RH, Kent WB, Radavich JF, editors. Warrendale, PA: The Minerals, Metals & Materials Society, 245-273.

[2] Hyzak, DA, Bernstein IM. The Effect of Defects on the Fatigue Crack Initiation Process in Two P/M Superalloys: Part II. Surface-Subsurface Transition. Met. Trans. A 1982; 13A: 45-52.

[3] Jablonski, DA. The Effect of Ceramic Inclusions on the Low Cycle Fatigue Life of Low Carbon Astroloy Subjected to Hot Isostatic Pressing. Mat. Sci. Eng. A 1981; 48: 189-198.

[4] Banik A, Lindsley B, Mourer DP, Zimmer WH. Alternative Processing for the Production of Powder Metal Superalloy Billet. Advanced Materials and Processes for Gas Turbines: Proceedings of the International Conference. Fuchs G, James A., Gabb TP, McLean M, Harada H, editors. Warrendale, PA: The Minerals, Metals & Materials Society, 2003, 227-236.

[5] Huron ES, Roth PG. The Influence of Inclusions on Low Cycle Fatigue Life in a P/M Nickel-Base Disk Superalloy. Superalloys 1996: Proceedings of the Eight International Symposium on Superalloys. Kissinger RD, Deye DJ, Anton DL, Cetel AD, Nathal MV, Pollock TM, Woodford DA, editors, Warrendale, PA: The Minerals, Metals & Materials Society, 1996, 359-368.

[6] Roth PG, Domas PA. Practical Application of Probabilistic Lifing Methods to Powder Metal Aircraft Engine Components. Structures, Structural Dynamics, and

Materials Conference and Exhibit. Reston, VA: American Institute of Aeronautics and Astronautics, 1997, 959-972.

[7] Xie X, Zhang L, Zhang M, Dong J, Bain K. Micro-Mechanical Behavior Study of Non-Metallic Inclusions in P/M Disk Superalloy Rene 95. Superalloys 2004: Proceedings of the Tenth International Symposium on Superalloys. Green KA, Harada H, Howson TE, Pollock TM, Reed RC, Schirra JJ, Walston S, editors, Warrendale, PA: The Minerals, Metals & Materials Society, 2004, 451-458.

[8] Cary PE. History of Shot Peening. Proceedings of the 1st International Conference on Shot Peening, Paris, France, 1981, 23-28.

[9] Gabb TP, Bonacuse PJ, Ghosn L, Sweeney JW, Chatterjee A, Green KA. Assessment of Low Cycle Fatigue Behavior of Powder Metallurgy Alloy U720. Fatigue and Fracture Mechanics: 31st Volume, ASTM STP 1389. Halford GR, Gallagher JP, West J, editors, Conshohocken, PA: American Society for Testing and Materials, 2000, 110-127.

[10] Gabb TP, Telesman J, Kantzos PT, Bonacuse PJ, Barrie RL. Initial Assessment of the Effects of Nonmetallic Inclusions on Fatigue Life of Powder-Metallurgy-Processed Udimet 720. Advanced Materials and Processes for Gas Turbines: Proceedings of the International Conference. Fuchs G, James A., Gabb TP, McLean M, Harada H, editors. Warrendale, PA: The Minerals, Metals & Materials Society, 2003, 237-244.

[11] Kantzos PT, Barrie RL, Bonacuse PJ, Gabb TP, Telesman J. The Influence of Forging Strain on Ceramic Inclusions in a Disk Superalloy. Advanced Materials and Processes for Gas Turbines: Proceedings of the International Conference. Fuchs G, James A., Gabb TP, McLean M, Harada H, editors. Warrendale, PA: The Minerals, Metals & Materials Society, 2003, 245-254.

[12] Bonacuse PJ, Kantzos PT, Telesman J, Gabb TP, Barrie RL. Modeling Ceramic Inclusions in Powder Metallurgy Alloys. Fatigue 2002: Proc. of the 8th Int. Fatigue Congress. A. F. Blom, editor. V. 2, 2002, 1339-1346.

[13] Gabb TP, Telesman J, Kantzos PT, O'Connor K. Characterization of the Temperature Capabilities of Advanced Disk Alloy ME3. NASA/TM-2002-211796. Washington, D.C.: National Aeronautics and Space Administration, 2002.

[14] Prevey PS. X-Ray Diffraction Residual Techniques. Metals Handbook 9th ed., Metals Park, OH: American Society for Metals, 1986, 80-392.

[15] Kantzos PT, Bonacuse P, Telesman J, Gabb TP, Barrie R, Banik A. Effect of Powder Cleanliness on the Fatigue Behavior of Powder Metallurgy Ni-Disk Alloy Udimet 720. Superalloys 2004: Proceedings of the Tenth International Symposium on Superalloys. Green KA, Harada H, Howson TE, Pollock TM, Reed RC, Schirra JJ, Walston S, editors, Warrendale, PA: The Minerals, Metals & Materials Society, 2004, 409-417.

[16] Prevey PS, Hornbach DJ, Mason PW. Thermal Residual Stress Relaxation and Distortion in Surface Enhanced Gas Turbine Engine Components. Proceedings of the 17th Heat Treating Society Conference and Exposition and the 1st International Induction Heat Treating Symposium. Milam DL, et al, editors. Materials Park, OH: American Society for Metals, 1998, 3-12.

[17] Gabb TP, Telesman J, Kantzos PT, Bonacuse PJ, Barrie RL, Hornbach DJ. Stress Relaxation in Powder Metallurgy Superalloy Disks. TMS Letters 2004; 5: 115-116.

[18] Grieving D, Gorelik M, Kington H. Manufacturing Related Residual Stresses and Turbine Disk Life Prediction. Review of Quantitative Nondestructive Evaluation, Vol. 24. Thompson DO, Chimenti DE, editors. Melville, NY: American Institute of Physics, 2005, 1339-1346.

Table I: Specimen Gage Section Dimensions.

	Length [cm]	Diameter [cm]	Surface Area [cm^2]	Volume [cm^3]
Unseeded	1.91	0.64	3.8	0.6
Seeded	3.18	1.0	10.13	2.57

Table II: Shot Peening Condition Screening Test Matrix.

Intensity	Coverage				
	200%	400%	500%	600%	800%
4A	X				X
6A		X	X	X	
8A	X				X

Table III: Regression Results of Screening Test Data.

Variable	Relationship	n	res DoF	RMS error	$R^2_{adj.}$
Surface Stress [MPa]	$-950.1+33.75I'$	12	10	42	0.28
Depth of Compressive Stress [μm]	$182.6+23.9I'+14.8D'$	12	9	11.9	0.81
Laps per cm of Surface Length [laps/cm]	$30.44+15.20I'+6.6C'+6.8D'+6.0I'C'$	9	4	3.30	0.97
Inclusion Exposed Surface Area Ratio [After/Before]	$0.38-0.16I'-0.17C'$	54	51	0.266	0.15
Surface Half Width	$5.59+0.23C'$	12	10	0.25	0.36
-270 seeded log(life)	$4.211-.037C'$	8	6	0.107	0.19
-150 seeded log(life)	$3.739-.2005I'C'$	9	7	0.25	0.77

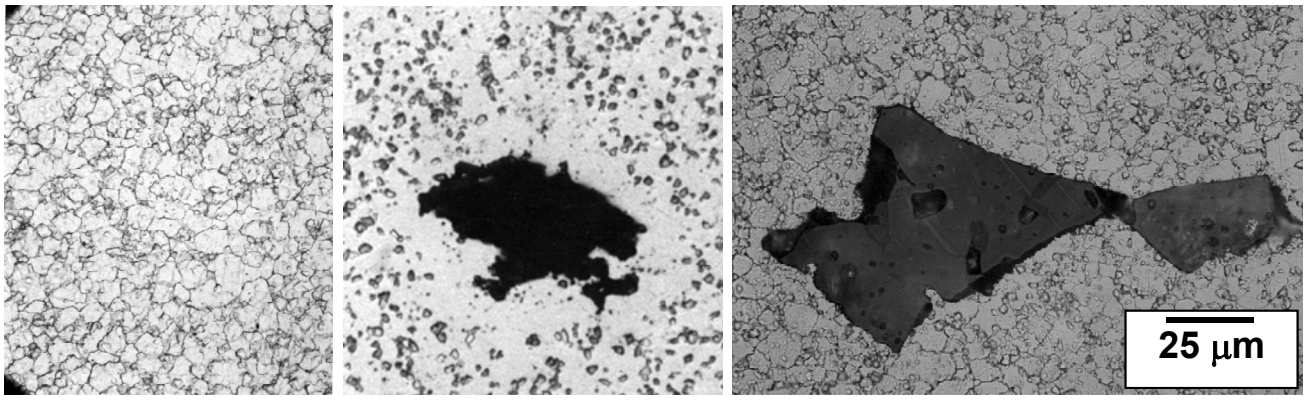

(a) (b) (c)

Figure 1: Typical microstructure of the (a) unseeded, (b) 54 μm seeded, and (c) 122 μm seeded disk forgings.

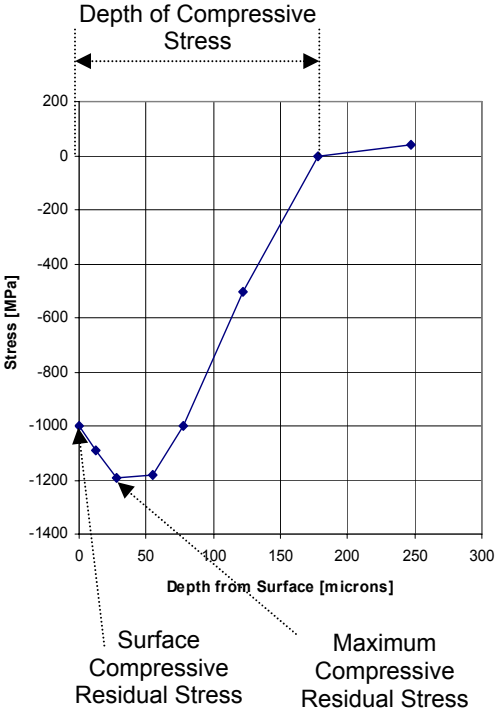

(a)

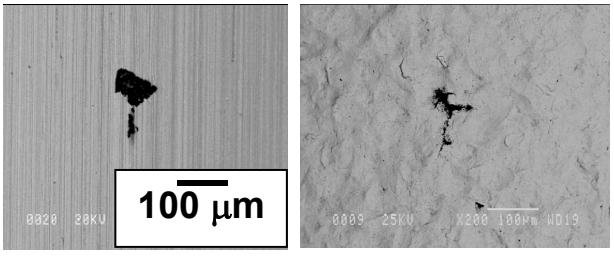

Pre-peening Area Post-peening Area

(b)

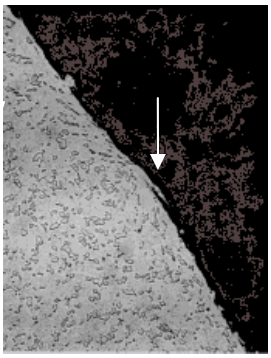

Lap

(c)

Figure 2: (a) Representative plot residual stress profile with definitions of measured parameters, (b) inclusion intersecting the specimen surface before and after shot peening, (c) transverse metallographic section showing a lap due to shot peening

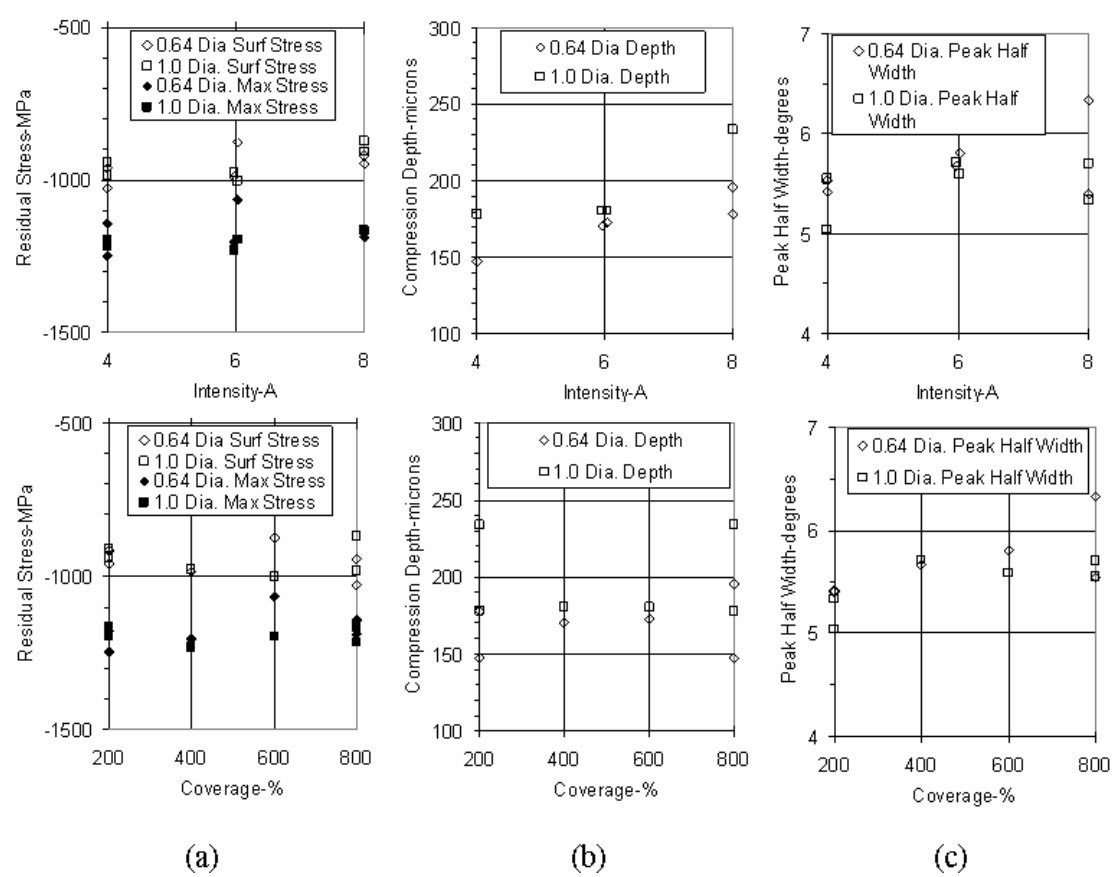

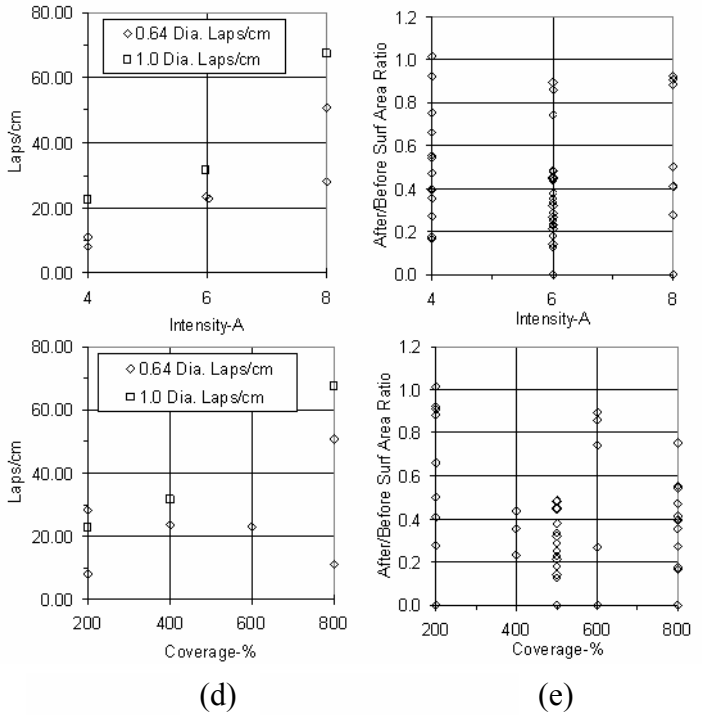

Figure 3: Simple scatter plots of (a) surface and maximum residual stresses, (b) depth of compression, (c) peak half width, (d) laps per cm of surface length, and (e) inclusion surface area ratio after/before shot peening.

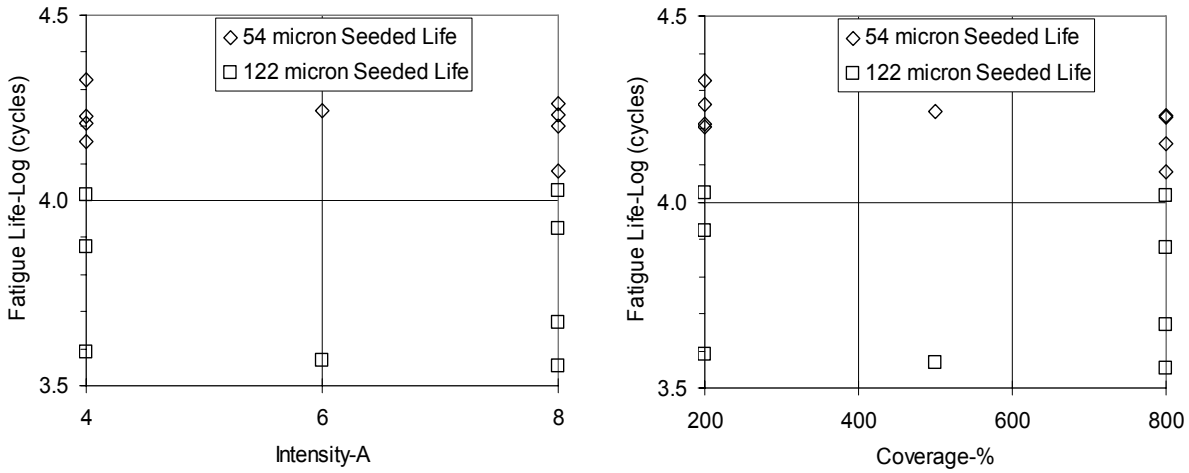

Figure 4: Fatigue life versus intensity and coverage for seeded specimens,

T=650°C, $\Delta\varepsilon_t$=0.8%.

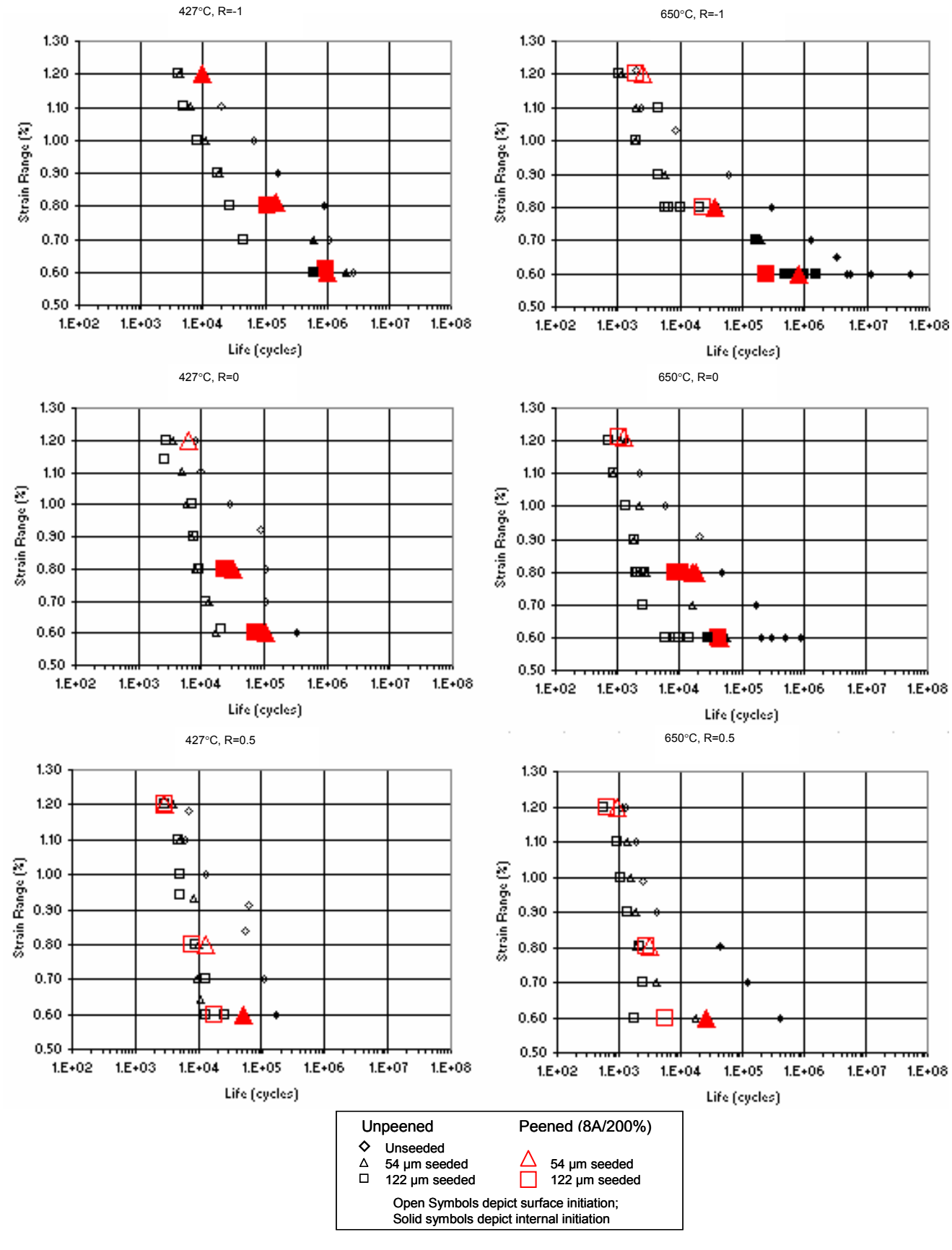

Figure 5: Strain life response of unseeded, 54 µm seeded, and 122 µm seeded Udimet 720.

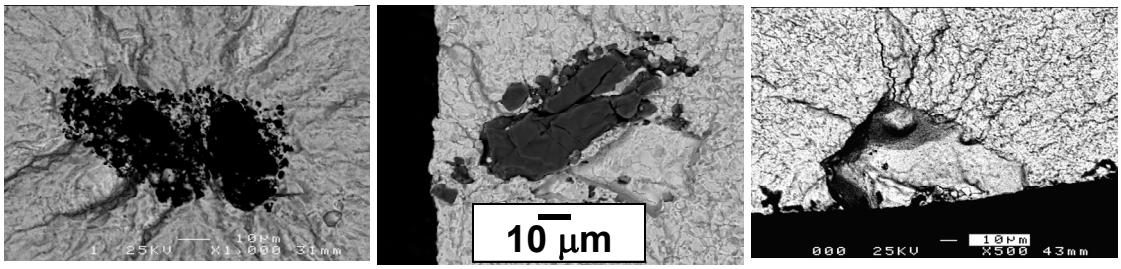

(a) (b) (c)

Figure 6: Representative fractography of unpeened specimens (a) unseeded, (b) 54 μm seeded, and (c) 122 μm seeded, T=650°C, $\Delta\varepsilon_t$=0.8%, R_ε=0.5.

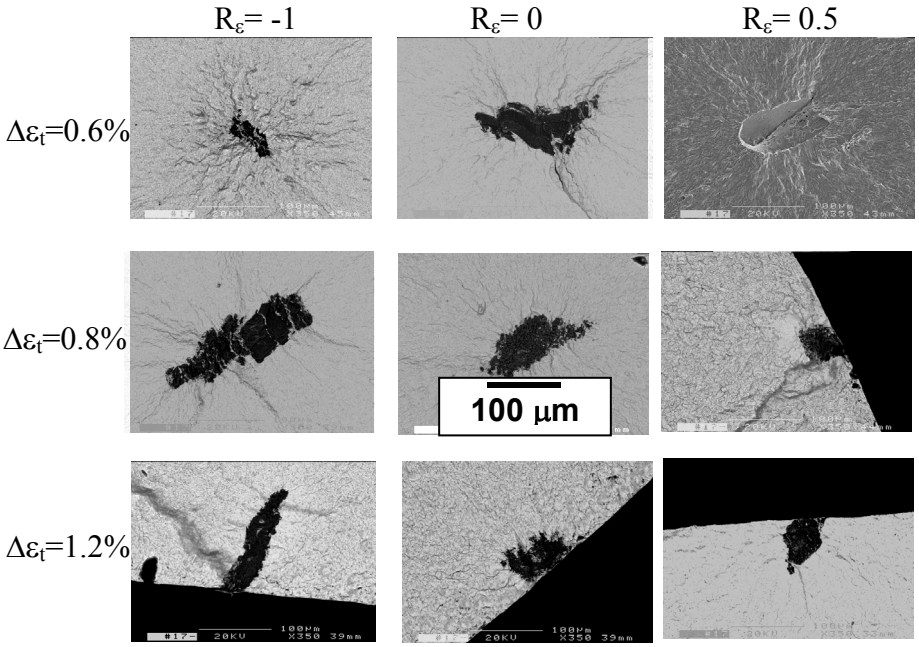

Figure 7: Representative fractography of 8A/200% peened, 54 μm seeded specimens, T=650°C.

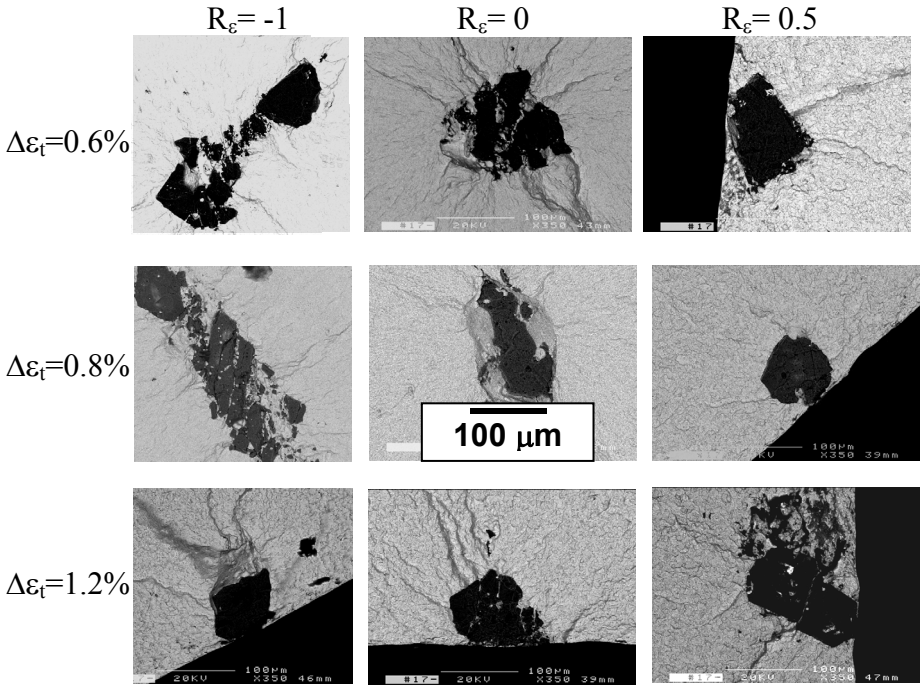

Figure 8: Representative fractography of 8A/200% peened, 122 μm seeded specimens, T=650°C.

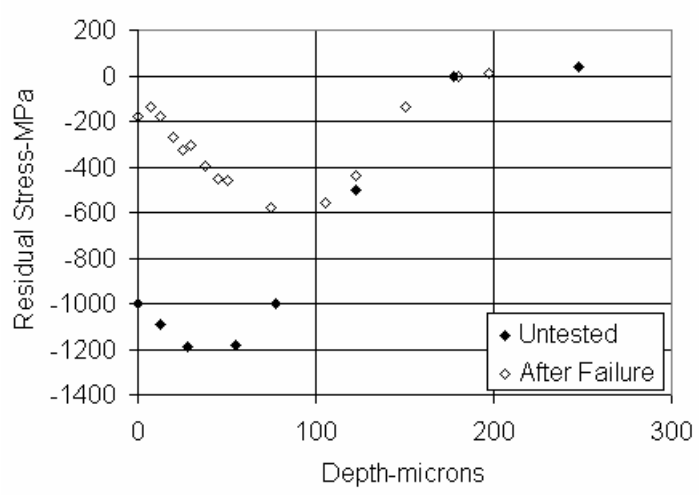

Figure 9: Axial residual stresses of shot peened specimen before and after testing at 650°C, 0.8% and R_ε=0.